Mechanisms of Interaction in IVT

R. FUCHS Y. HASUDA

The torque controlled full toroidal IVT (Infinitely Variable Transmission) is known to give significant fuel consumption benefits compared with conventional stepped ratio transmissions. Those benefits are obtained in part by achieving high overdrive (low engine speed at high vehicle speed) while ensuring good driveability. To achieve this driveability, the system is required to have fast response while being well damped and stable. The objective of this paper is to give a theoretical overview of the two main mechanisms of interaction in the IVT. The concept of stability is applied on each subsystem then on their interactions to define design requirements for proper system response. This analysis is built on previous work on variator modeling[1] and validation[2].

***Key Words**: IVT, torque control, stability, performance, interaction*

1. Introduction

One of the main requirements to achieve low fuel consumption is to operate a driveline at high overdrive. This means that the engine should operates at low rotational speed while the vehicle has a high velocity. In this situation, excellent driveability should be ensured. Driveability can be qualified in terms of system response, damping and stability.

A torque controlled full toroidal IVT driveline offers many advantages to achieve those requirements. The full toroidal variator has the widest ratio range of all CVT (Continuously Variable Transmission). It is torque controlled instead of the conventional ratio control providing faster response. On the other hand, two main interactions affect the IVT. They are the variator-hydraulic control circuit interaction and the variator-driveline interaction. Both must be fully understood to achieve proper system design and good dynamic performances.

2. Approach

This analysis is based on previous work on variator and IVT driveline modeling, and on variator model validation[1), 2)]. The approach followed here consists first in analyzing the variator frequency response. Then two generic hydraulic control circuits are introduced and their interactions with the variator discussed. Finally, a simplified driveline model is developed and the variator-driveline interaction is analyzed. **Figure 1** gives an overview of the two interactions with the variator.

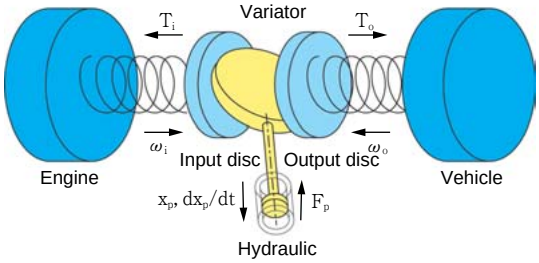

Fig. 1 Overview of IVT interactions

3. Concept of Stability

This paragraph aims at giving a brief overview of the mathematical concepts used to describe stability in this paper. This work deals with nonlinear SISO (Single-Input, Single-Output) and MIMO (Multiple-Input, Multiple-Output) systems whose nonlinearities can be classified as "soft". This justifies the use of well-known linear techniques such as linearization and frequency analysis for the investigation of the IVT interactions.

3. 1 Internal Stability

Internal stability is a concept related to linear SISO and MIMO systems in the form

$$\begin{aligned} \dot{x}(t) &= Ax(t) + Bu(t) \\ y(t) &= Cx(t) + Du(t) \end{aligned} \qquad (1)$$

The state-space form gives access to internal variables or states $x(t)$ of the system regardless of its input and output. The internal stability is demonstrated if all eigenvalues of the matrix A are strictly in the left-half of the complex plane[3].

3. 2 BIBO Stability

The concept BIBO (Bounded Input Bounded Output) stability states that a linear time invariant (LTI) SISO system is BIBO stable if all bounded inputs generate bounded outputs.

The BIBO stability is inherently an external concept where only input and output are concerned. LTI SISO systems described by rational transfer functions are BIBO stable if and only if all poles are strictly in the left half of the complex plane[4].

In some limits, if a system is proved to be internally stable, it is BIBO stable as well.

4. Frequency Response of the Full Toroidal Variator

4. 1 Overview of the Variator

The main subsystem of the IVT is the torque controlled full toroidal variator. The variator behavior is dictated by two mechanisms: *traction drive*, which permits transmission of power through loaded contacts between smooth surfaces and the *steering geometry* or *castor angle* of the roller carriage, which enables self-alignment of the rollers. The complex dynamic of the variator is the results of the combination of these two mechanisms in the toroidal shape of the cavities formed by an input and an output discs where the rollers evolve. **Figure 2** gives an overview of the full toroidal variator.

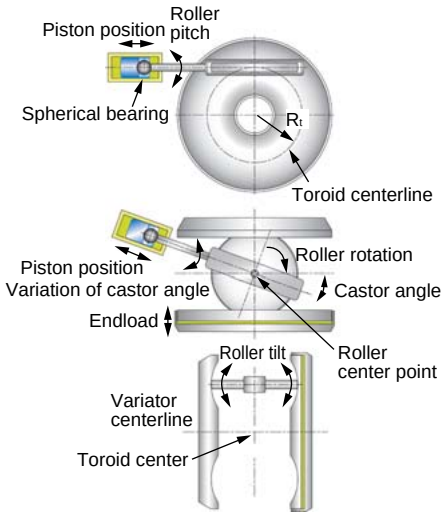

Fig. 2 Variator geometry and roller dof (The full toroidal variator is composed of 2 cavities with 3 rollers each)

4. 2 Input Boundaries

The variator is a nonlinear MIMO system, which comprises 4 inputs (input speed, output speed, endload force and piston force) and 4 outputs (input torque, output torque, piston position and piston velocity). Proper operation of the variator imposes bounded inputs that represent the working frame:

- Input speed (ω_i) is bounded between 0 and the engine maximum speed multiplied by the input gearing speed ratio.
- Output speed (ω_o) is bounded between minimum and maximum variator ratio.
- Endload force (F_e) is bounded by the endload spring, which provides a pre-load (not depicted in **Fig. 2**) and the maximum pressure of the hydraulic circuit.
- Piston force (F_p) is bounded between 0 and a maximum value corresponding usually to the cracking pressure of a relief valve.

Physical limitations are defined with the contact power capacity, material resistance and durability. Additional restrictions on coupled inputs must be considered as well. The input and output speeds are coupled by the ratio spread of the variator as mentioned above but also their directions are defined with the sign of the castor angle. The forces are coupled to ensure good traction conditions. A steady state control law can be obtained considering the forces equilibrium on a roller and small angle.

$$\frac{F_p}{F_e} = \frac{2}{3}\,\frac{\mu}{\cos(\beta)} \qquad (2)$$

where μ is the traction coefficient and β the castor angle.

4. 3 Model Linearization and Stability

The full toroidal variator model described in[1] has 5 states: roller speed, piston position, piston velocity, tilt angle and tilt speed. Linearization of this nonlinear MIMO model can be performed symbolically or using numerical computation. Both ways were developed for consistency cross checking. Internal stability of the variator model has been checked computing the eigenvalues of the matrix A over the whole inputs ranges.

4. 4 Frequency Response

The two Bode plots of concern for variator interaction analysis are shown in **Fig. 3**. The input or output torque versus input or output speed (T_i/ω_i or T_o/ω_o) transfer function is useful for the variator-driveline analysis and the piston velocity versus piston force ($dx_p/dt/F_p$) for the variator-hydraulic interaction. A new input limitation can be defined here as the maximum rate of speed change. This rate is limited by traction as it changes the contact slip. Although this limitation does not affect the numerically computed Bode diagrams, as long as the amplitude of the speed perturbation signal is smaller than the maximum acceptable slip, it should be considered as a nonlinear system limitation. Using time domain simulation, the maximum speed change rate has been estimated above 1 kHz, which is much higher than conventional driveline bandwidths.

The variator Bode diagrams feature one resonance peak due to the steering geometry at about 30 Hz. The peak indicates an under damped dynamics of the variator. The resonance should be considered with care, as it may be critical when interactions with other subsystems appear in its neighborhood. Therefore, in depth investigation of the parameters and inputs that affect this peak should be carried out. Further interpretation of the variator frequency response can be resumed as follows. The general "high-pass" tendency of the torque/speed response comes from the traction. At low frequency, the disc speed change is too slow to cause a slip change. The roller merely follows. However, for fast speed change, slip increases producing higher traction coefficient and therefore higher torque. The same explanation holds for the piston speed versus piston force transfer function.

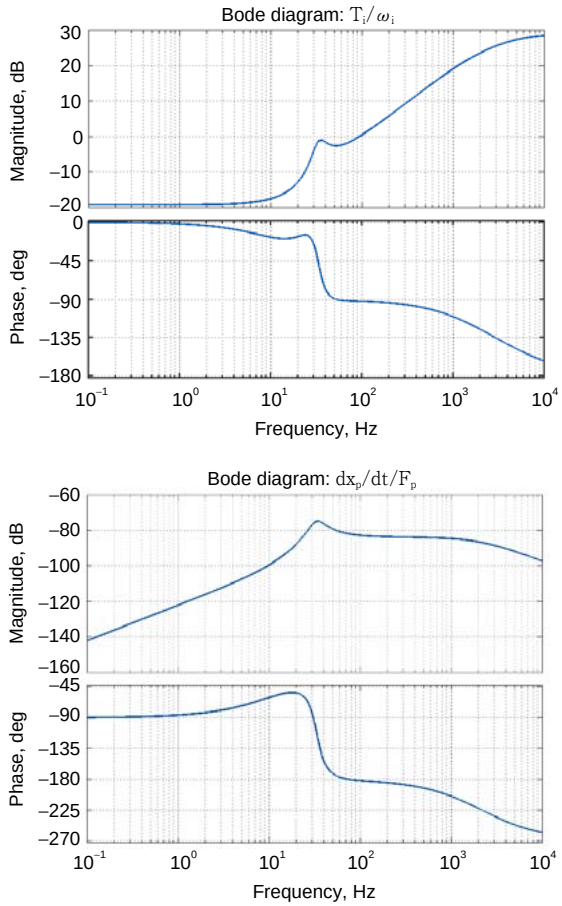

Fig. 3 Bode diagrams of the full toroidal variator transfer functions T_i/ω_i and $dx_p/dt/F_p$, linearized at the working point $\omega_{i0} = 200$ rad/s, $i_{var0} = -1$, $F_{e0} = 47.5$ kN and $F_{p0} = 1.5$ kN

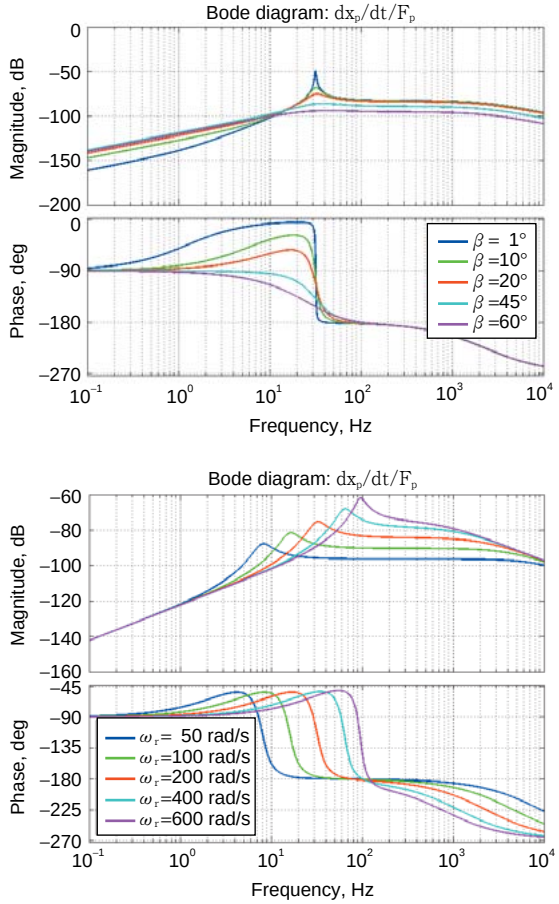

Fig. 4 Damping effect of the castor angle and stiffness effect to the roller speed

4. 5 Parametric Study

The notion of parametric study of linear system should be extended for nonlinear system as to include the effect of the working point. This means that the frequency response depends not only on the system parameters but also on its inputs level. The dominant parameters were identified to be the castor angle and the roller speed. This is based on the assumption that the roller mass is small enough to neglect inertia effect. The castor angle has a dominant effect on variator damping while the roller speed on variator stiffness (**Fig. 4**). In fact, the resonance frequency is equivalent to the roller speed. Although castor angle is a system parameter therefore fixed by design (currently 20°), roller speed is a state dependent on discs speeds. Thus, the resonance frequency is continuously changing. In **Fig. 4**, the resonance frequency varies from about 8 to 95 Hz. The frequency range of the resonance peak should be considered for the analysis of the interactions with the variator and as a design restriction of the hydraulic circuit.

5. Interaction Variator-Hydraulic

Current solution to generate endload and piston forces uses hydraulic power. Basic requirements of the hydraulic control circuit are to provide endload and piston pressures satisfying the control law (2) and an actuation (solenoid valve) for piston pressure control. The analysis of the interaction variator-hydraulic concerns only the piston force or pressure. The endload actuation is assumed ideal.

The mechanism of variator interaction can be resumed as follows: consider the variator at steady state, a pressure demand is set on hydraulic actuators, usually solenoid valves. If the engine speed suddenly changes, it will cause the variator ratio to change inducing a roller motion. The associated piston translation will induce a flow or pressure perturbation in the hydraulic circuit affecting the pressure demand. Because of the proportional relationship piston pressure or force to torque, the load on the engine respectively the torque on the wheels will change causing potential engine respectively wheel speed variation and so on. The hydraulic interaction corresponds to the part where piston motion produces a pressure perturbation affecting the variator. **Figure 5** gives an illustration of this interaction.

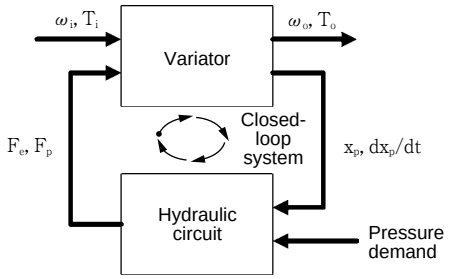

Fig. 5 Interactions between variator and hydraulic system

5. 1 Pressure Control Circuit

Two generic pressure control circuits are considered as they cover a wide range of possible solutions for torque controlled variator actuation. They are based on two different types of valve: flow control valve and pressure-reducing valve (**Fig. 6**). The first features a spool position dependent on control current only. The second has a spool which position depends on control current and pressure (pressure feedback).

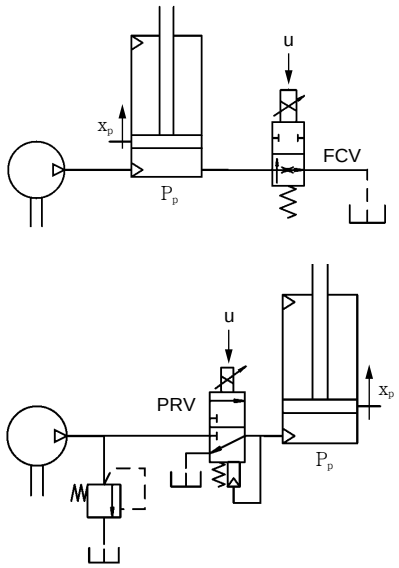

Fig. 6 Pressure control circuits based on a flow control valve (FCV) and on a pressure-reducing valve (PRV)

Using flow control valve for pressure control is not conventional. Despite, disadvantages such as the nonlinear pressure/control current relation and spool stiction, flow control valves can be very simple and spool position or orifice area are directly related to the control current. The spool position is therefore independent on pressure changes. This is an advantage for variator stability, as pressure perturbation will not cause spool oscillations. The hydraulic concept shown in **Fig. 6** uses a pump to deliver a constant flow to the circuit while the valve defines the circuit pressure.

Bode diagram of the transfer function force versus piston velocity ($F_p/dx_p/dt$) shows that the hydraulic circuit behaves merely like a low pass filter. The cut-off frequency depends on system parameters and on the load pressure (P_p). **Figure 7** depicts the frequency response of the hydraulic circuit for different pressure levels. This shows that for higher pressure, the static gain increases and the cut-off frequency decreases. Over the variator pressure range, the cut-off frequency varies from about 70 to 400 Hz.

BIBO stability of this circuit is straightforward and can be easily demonstrated algebraically.

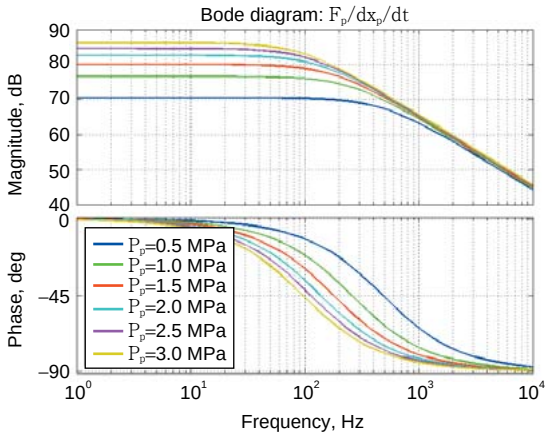

Fig. 7 Bode diagram of the transfer function piston force/speed of the FCV-based hydraulic circuit

The pressure-reducing valve features a proportional control of the pressure over solenoid current and low hysteresis. Although these characteristics are better than the flow control valve in terms of variator actuation, spool position is sensitive to pressure. This means that interaction between variator and hydraulic will cause spool oscillations. The circuit concept shown in **Fig. 6** uses a pump connected to a relief valve to act as a constant pressure source. The pressure-reducing valve connected between the pressure source and the piston permits to control the piston pressure.

Bode diagram is shown in **Fig. 8**. Fundamental difference compared to the circuit using flow control valve appears as the pressure-reducing valve has a resonance peak. Although, the resonance frequency and magnitude depends on the valve design, the dominant parameter for a given valve is the load compliance. Small volume or high bulk modulus makes the circuit stiffer and therefore less damped. Furthermore, the resonance frequency appears to be in within the frequency range of the variator resonance. Although, the oscillatory behavior of the pressure-reducing valve is not a problem specific to the IVT, careful design should be made, using for example well-known compliance valve to avoid any possible hydraulic instability.

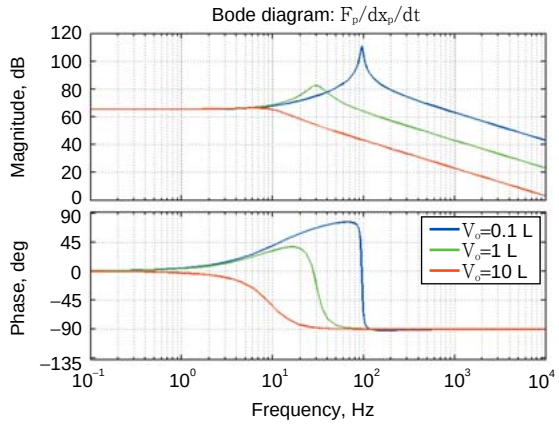

Fig. 8 Bode diagram of the transfer function piston force/speed of the PRV-based hydraulic circuit

5. 2 Variator and Flow Control Valve

Connection of the variator with the flow control valve based hydraulic circuit shows no concern in terms of stability. **Figure 9** shows variator-hydraulic closed-loop responses of the piston velocity at different disc speeds. The main effect of the hydraulic circuit is of damping nature. The resonance still follows the roller speed but its gain is attenuated and its phase transition smoothed. The reason is that as the disc speed increases the variator resonance peak is moving toward the hydraulic cut-off frequency causing attenuation of the variator response.

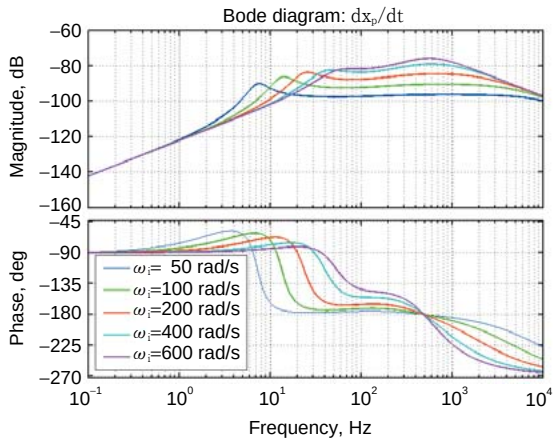

Fig. 9 Piston velocity closed-loop transfer function of the FCV-based circuit. The variator working point is set to $i_{var0} = -1$ and $P_{p0} = 2\ MPa$ and $V_0 = 1\ L$

5. 3 Variator and Pressure-Reducing Valve

Appropriate choices during hydraulic design can achieve stability without problem. Nevertheless, the pressure reducing valve case is interesting as it highlights the importance that every part affects system performance. Thus, parts or components design should satisfy system stability and offer proper system behavior and response. This hydraulic circuit also produces hydraulic damping. The reason is the same than for the flow control valve based circuit. As disc speed increases, variator resonance peak moves toward the resonance peak of the hydraulic circuit. **Figure 10** depicts clearly the two peaks. The resonance from the hydraulic circuit is fixed at 30 Hz and the variator peak moves from 7 to 100 Hz. Because hydraulic compliance is high enough, the interaction is stable in all situations.

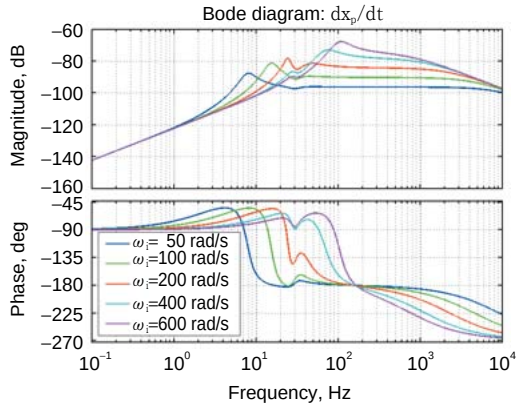

Fig. 10 Piston velocity closed-loop transfer function of the PRV-based circuit. The variator working point is set to $i_{var0} = -1$ and $P_{p0} = 2\ MPa$ and $V_0 = 1\ L$

6. Interaction Variator-Driveline

The second main interaction seen by the variator is of mechanical nature. It appears at both input and output sides of the variator when connected to inertia, like the engine and the wheels, through compliant shafts (**Fig. 1**). In fact, the variator couples the engine inertia with the vehicle inertia. **Figure 11** illustrates the closed-loop formed when connecting the variator with the driveline.

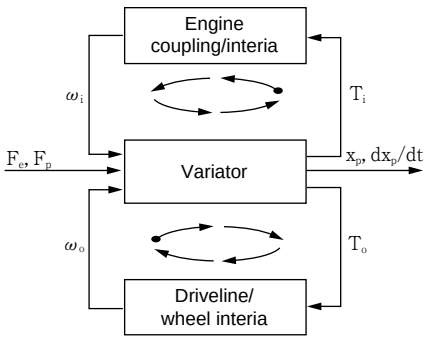

Fig. 11 Variator-driveline interaction

6. 1 Fundamental Mechanism of Interaction

A simplified shaft-inertia model is used to describe the driveline in order to avoid complex mathematical development and to highlight the basis of the interaction variator-driveline. This model consists of a driveline reduced to an equivalent inertia (I), an equivalent stiffness (k) and damping (c) of a compliant shaft. Assuming engine and vehicle speed constant, the transfer function speed versus torque can be written

$$\frac{\omega_{i,o}}{T_{i,o}} = \frac{s}{Is^2 + cs + k} \qquad (3)$$

Stability is demonstrated computing the root of the denominator. As all parameters are strictly positive, the shaft-

inertia system is unconditionally stable. Marginal stability is obtained in the unrealistic situation where the damping coefficient is null.

Frequency response of this transfer function is shown in **Fig. 12** for different damping coefficients. This response features a resonance peak for low damping values.

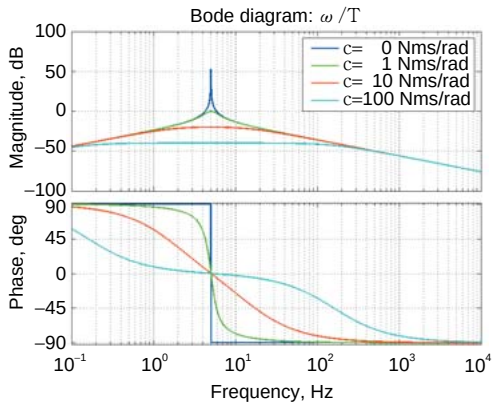

Fig. 12 Bode diagram of speed versus torque of a shaft-inertia model with $I = 0.1\ kgm^2$, $k = 100\ Nm/rad$

6. 2 Variator and Simplified Driveline

The resonance of the shaft-inertia model is located at a frequency within the frequency range of the variator resonance. However, because the shaft-inertia transfer function gain remains negative, the interaction is stable. **Figure 13** shows the open-loop speed response of the variator connected to the simplified driveline with a damping null and for different speeds. This represents a worst-case situation because damping coefficients are difficult to estimate and vary with temperature and life. The responses show a peak at 5 Hz due to the driveline resonance. The variator resonance follows speed. At 50 rad/s variator and driveline resonance are aligned causing the response gain to rise above 0 dB while its phase remains in the unstable region. This imposes the hydraulic control circuit to be designed to supply the necessary phase margin and provide sufficient damping in the driveline.

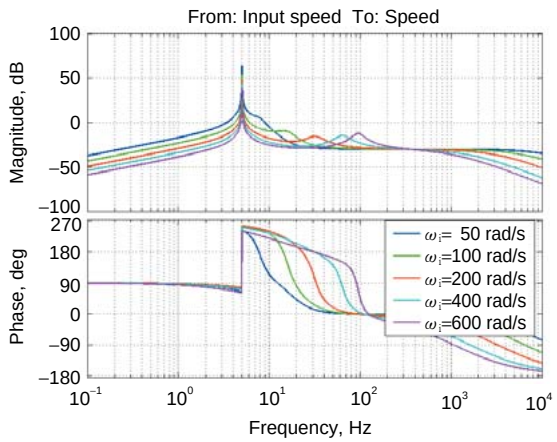

Fig. 13 Bode diagram of the open-loop transfer function of variator-driveline. The working point is set to $i_{var0} = -1$, $P_{p0} = 2\ MPa$, $I = 0.1\ kgm^2$, $k = 100\ Nm/rad$ and $c = 0\ Nms/rad$

Thus, it appears that the system variator-shaft-inertia is basically stable except for exceptionally low torsional damping factor, which are unrealistic. However, consideration of null damping is required for robust system design.

7. Conclusion

This investigation on the basic mechanisms of interaction of a full toroidal IVT driveline is a key step in a theoretical approach of system design. The stability of each subsystem has been demonstrated. This allowed a more in depth investigation of these subsystems performances resulting in an identification of the dominant parameters. Variator-hydraulic and variator-driveline interactions were investigated. Two generic hydraulic circuits were considered. They showed to have mainly a damping effect on the variator response. A simplified driveline model was used to point out the fundamental of its interaction with the variator. This has permitted to identify key requirements for the hydraulic design.

References

1) R. D. Fuchs, Y. Hasuda, I. B. James, Full Toroidal IVT Variator Dynamics, SAE paper 2002-01-0586, March 2002.
2) R. Fuchs, Y. Hasuda, I. B. James, Modeling, Simulation and Validation for the Control Development of a Full-Toroidal IVT, CVT2002 Congress, VDI-Berichte 1709, October 2002.
3) R. Vaccaro, Digital Control: a State-Space Approach, Mc Graw-Hill, 1995.
4) R. Longchamp, Commande Numerique de Systemes Dynamiques, PPUR 1995.

R. FUCHS* Y. HASUDA*

* *Mechatronic Systems Research & Development Department, Research & Development Center*